FISEVIER

Contents lists available at ScienceDirect

Applied Thermal Engineering

journal homepage: www.elsevier.com/locate/apthermeng



Research Paper

Natural convection effect on heat transfer in saturated soils under the influence of confined and unconfined subsurface flow

Fereydoun Najafian Jazi, Omid Ghasemi-Fare, Thomas D. Rockaway

Department of Civil and Environmental Engineering, University of Louisville, Louisville, USA

ARTICLE INFO

Keywords: Soil hydro-thermal response Heat transfer Natural convection Groundwater flow Mixed convection

ABSTRACT

Recently, it has been proven that natural convection significantly impacts heat transfer close to geothermal systems in saturated soils even in the presence of groundwater flow. However, this phenomenon has only been investigated in the presence of confined groundwater flow. Therefore, in this study, a fully coupled hydrothermal model was developed to quantitatively determine the natural convection influence on heat transfer in the presence of an unconfined groundwater flow and to compare the hydro-thermal response of soil under these two different scenarios. Results showed that natural convection influence depends on the coupled effects of soil permeability, groundwater velocity, and heater temperature. According to the results, in the case of a groundwater flow velocity less than 10^{-7} m/s, natural convection role is non-negligible when Rayleigh number is greater than 50, while for other groundwater velocities, that matters only when Buoyancy ratio is greater than 20. It was also shown that choosing a confined groundwater flow over an unconfined one led to an error of 47 % to 173 % in the explored scenarios. Furthermore, it was revealed that when the relative distance of the heater from the surface alters from 0 to 15 and 30 m, the error in the soil temperature due to neglecting natural convection can be as high as 43 %, 48 %, and 60 %, respectively.

1. Introduction

Geothermal energy systems are proving to be sustainable and environmentally friendly systems with significant potential to help meet future energy demands. These systems utilize heat exchangers installed in the ground to inject/harvest thermal energy to/from the ground in order to partially heat or cool the built environment [12]. Most commonly, geothermal systems are used to help maintain constant temperatures within building envelopes [24,50], however, they can be used in a variety of applications such as helping to prevent thermal cracking of pavements caused by seasonal temperature fluctuations [34]. More recently, they have been used for energy storage purposes, where thermal energy is stored close to borehole heat exchangers for future applications [6]. Given that the performance of such systems heavily relies on changes in ground temperature, a precise assessment of soil thermal response within the influence zone is crucial for optimizing the efficiency of geothermal energy systems [23].

Several numerical and analytical studies have previously investigated the soil thermal response close to an embedded heat source (e.g., a geothermal pile). The majority of this research has considered

conduction the sole heat transfer mechanism as [1,11,17,19,21,31,32,38,40]. However, a few studies have reported that natural convection can significantly change the temperature distribution close to the heat source [41,45,46,51]. Natural convection, also known as thermally induced fluid flow, is a fluid flow that is driven by buoyancy. When heated, the density gradient in the fluid rises due to temperature variations within the heated zone. Sharqawy et al. [43] showed that considering natural convection within a thermal system can reduce the required length of the geothermal borehole by up to 50 % in soils with a permeability of 5×10^{-9} m². Ghasemi-Fare and Basu [22], concluded that even under hydrostatic conditions, soil thermal response can only be accurately predicted by combining the effects of both heat conduction and heat convection [23]. Bidarmaghz and Narsilio [9] work supported these findings when they numerically explored the influence of natural convection on deep borehole heat exchangers' performance. Results of their analysis revealed that consideration of natural convection increased the thermal efficiency of the borehole heat exchangers with different lengths of 2, 3.5, and 5 km respectively by up to 63, 53, and 43 % compared to the cases that neglected the natural convection.

In addition to conduction and natural convection, the presence of groundwater flow and the resulting forced convection can significantly

E-mail addresses: fereydoun.najafianjazi@louisville.edu (F. Najafian Jazi), omid.ghasemifare@louisville.edu (O. Ghasemi-Fare), tom.rockaway@louisville.edu (T.D. Rockaway).

^{*} Corresponding author.

affect the temperature distribution in the soil [13,14,16,18,25,31,35,48,52]. Wang et al. [49] experimentally measured the heat injection rate of a borehole heat exchanger in Baoding, China, in the presence of a 0.96×10^{-6} m/s groundwater flow and reported that the heat transfer rate was improved by about 9.8 % due to the groundwater flow. In another experimental study, Sun et al. [44] evaluated the heat transfer in a saturated porous medium in the presence of subsurface flow during thermal conduction heating (TCH), as a thermal treatment technique. The evaluation of isothermal contours after 360 min of heating showed that an increase in the groundwater velocity from 0 to 9.51×10^{-9} , 2.06×10^{-8} and 3.17×10^{-8} m/s (from 0 to 0.3, 0.65, 1 m/year) resulted in a propagation of the thermal influence zone by 0.06, 26.55, and 29.55 %, respectively. Cai et al. [10] developed an analytical solution by combining composite medium linesource (CMLS) and moving line-source (MLS) methods to investigate heat transfer in borehole heat exchangers in the presence of groundwater flow. Based on their results, the borehole circulating fluid temperature dropped by 30 % when the groundwater flow was equal to 2 \times 10⁻⁶ m/s compared to the no-groundwater flow condition in the longterm (after 150 days of heating).

Despite numerous studies investigating the impact of subsurface flow on heat transfer in the vicinity of an embedded heat source in saturated soils, only a limited number of studies have considered the combined influence of natural and forced convection (mixed convection) on heat transfer [33,42,47]. Tiwari and Basu [47] recently conducted a finite element analysis to investigate the effect of mixed convection in the vicinity of a geothermal pile. They observed that, in a medium with a permeability of $5 \times 10^{-9} \, \text{m}^2$ and in the presence of the groundwater flow with a velocity ranging from 0 to 10^{-6} m/s, the effective thermal conductivity increased by up to 36 % when mixed convection was considered, compared to the case that only accounted for conduction. In another study, Mehraeen et al. [33] explored the combined effect of natural and forced convection in horizontally oriented-saturated ground. They demonstrated that in the case of high soil permeability (i.e., 10^{-9} m²), thermally induced fluid flow reduced the soil thermal response, even in the presence of high groundwater flow velocity (17.3

% reduction at a distance of 2 m downgradient from the heat source with a groundwater flow velocity of 10^{-6} m/s). Furthermore, they developed a non-dimensional parameter, as a function of soil permeability and heat source temperature, to assess the relative importance of natural convection at various radial distances. However, it should be noted that in their criterion, the effect of groundwater flow velocity was neglected, although they have demonstrated that the natural convection impact on heat transfer highly depends on the groundwater flow velocity (i.e., forced convection).

It is important to note that when considering natural convection, the buoyancy force induced by a temperature gradient tends to promote upward flow, resulting in the vertical transfer of thermal energy towards the surface [42]. In this situation, the hydraulic boundary condition on the surface becomes significantly important in determining the fluid flow direction and, consequently thermal energy distribution in shallow depths. As shown, existing literature on the mixed convection and natural convection has mainly investigated this context in the presence of confined groundwater flow, where the surface pressure differs from atmospheric conditions. In fact, the effect of boundary conditions on the hydro-thermal response of soil has been disregarded in the literature. However, soil hydro-thermal response may differ under the unconfined condition, where the fluid flow pattern close to the surface remains unchanged compared to the confined condition. Furthermore, the confined boundary condition is not realistic in most cases and fails to represent the subsurface conditions close to geothermal boreholes/piles or other embedded heat sources in the ground. Considering the significant research gap in the literature regarding this matter, further studies are necessary to scrutinize the role of natural convection in heat transfer in the presence of the unconfined groundwater flow and evaluate the changes in the direction of thermally induced pore water flow under confined and unconfined boundary conditions.

The current study hypothesized that the direction of natural convection highly depends on the surface boundary condition. Therefore, this paper aims to explore the effect of natural convection on soil hydrothermal response in a saturated porous medium under different hydraulic and boundary conditions. To achieve this, a three-dimensional

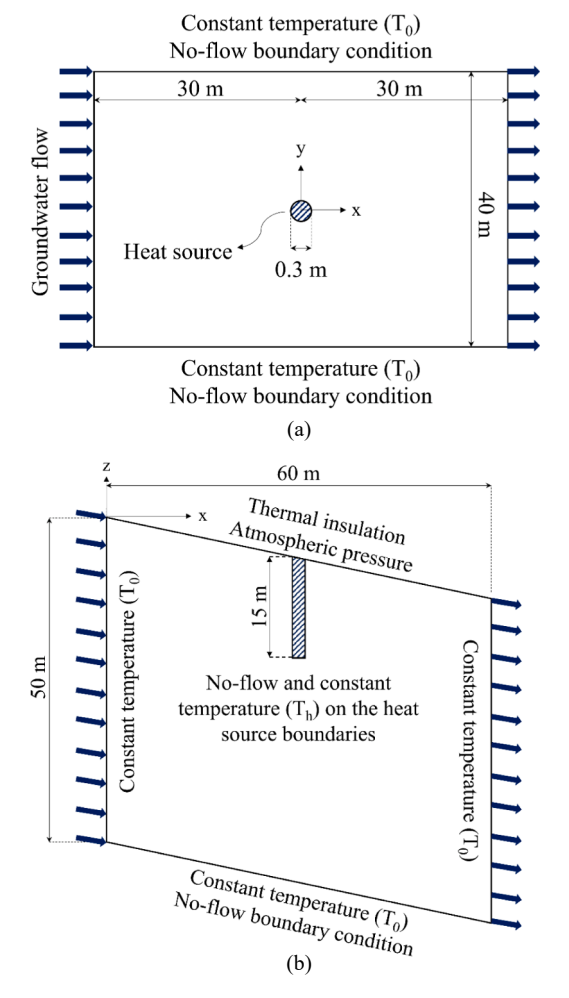


Fig. 1. Schematic of the model and boundary conditions in a) the horizontal and b) the vertical cross-section.

finite element (FE) model was developed in COMSOL Multiphysics to incorporate the thermal and hydraulic behavior of the porous medium. Unlike previous studies, in this model, an inclined ground was considered to simulate the unconfined groundwater flow resulting from an elevation gradient. Additionally, to the authors' knowledge, the literature lacks a precise criterion that could help researchers/designers decide what type of heat transfer mechanisms (i.e., conduction, forced convection, or natural convection) should be considered in different hydro-thermal conditions. By changing the soil permeability, the groundwater velocity, and the heat source temperature, a parametric study was conducted to observe the role of different heat transfer mechanisms, especially natural convection, in different conditions. Natural convection's influence on soil thermal response was quantitatively related to two non-dimensional numbers, buoyancy ratio (Co) and Rayleigh number (Ra). Furthermore, considering the vertical direction of natural convection flow and consequently, its role in heat transfer, the embedded depth of the heat source was altered in certain analyses to evaluate the influence of mixed convection on heat transfer near heat sources with different embedding depths. Please note this study attempted to expand the current understanding of soil hydro-thermal response adjacent to a vertical heat source embedded in the ground (such as a geothermal pile, power cable, or thermal conduction heating) to facilitate a more precise prediction of the ground temperature. It is expected that the results help researchers and engineers modify the existing approach to analyzing these systems.

Table 1 Model input parameters.

Parameter	Value
Heat source diameter (Dh)	0.3 m
Heat source length (Lh)	15 m
Initial ground temperature (T ₀)	15 °C
Heat source temperature (Th)	40–80 °C
Porosity (φ)	$0.35 \text{ m}^3/\text{m}^3$
Permeability (κ)	10^{-9} - 10^{-12} m ²
Density of solids (ρ_s)	2650 kg/m ³
Thermal conductivity of solids (k _s)	2.5 W/m/K
Thermal conductivity of water (k _f)	0.6 W/m/K
Specific heat capacity of solids (C _s)	810 J/kg/K
Specific heat capacity of water (C _f)	4200 J/kg/K
Dynamic viscosity of water (μ)	0.001 Pa s
Groundwater flow velocity (w)	10^{-6} - 10^{-9} m/s

2. Problem definition

2.1. Geometry and boundary conditions

As mentioned earlier, the present study investigates the thermal behavior of soil surrounding an embedded heat source under the influence of an unconfined subsurface flow and compares it with the model that considers confined groundwater flow. A 3D finite element model was developed using COMSOL Multiphysics. Various domain sizes were initially considered in the modeling. Ultimately, a domain size of 60 m \times 40 m \times 50 m was selected to reduce the influence of boundary conditions on the soil hydro-thermal response close to the heater. For simplicity, the heat source was considered as a cylinder (with a diameter of 0.3 m and a height of 15 m) with a constant temperature on the surface (T_h) (Fig. 1). It should be mentioned that this assumption is valid for long-term analyses as it only takes a few hours to a few days for the borehole heat exchanger to reach a constant temperature [20]. However, to analyze the short-term response, it is necessary to simulate the heat transfer in the borehole. In that case, the precise knowledge of borehole components' characteristics is essential as they play important roles in transferring thermal energy to the surrounding soil [5,7,37] which is beyond the scope of this study.

In order to simulate the unconfined groundwater flow, an inclined geometry was implemented in the model, resulting in different potential heads and a hydraulic gradient caused by topography. It should be noted that in case of an unconfined groundwater flow (i.e., considering atmospheric boundary conditions on the surface), it is essential that the hydraulic gradient should only be induced by topography. Otherwise, the fluid pressure on the surface will be different than atmospheric pressure and the groundwater flow will no longer be in an unconfined condition. Inflow and outflow velocities, aligned parallel to the ground surface and proportional to the slope of the ground, were applied at the left and right boundaries of the domain, respectively. While the other sides of the domain were set as no-flow boundary conditions. The surface of the ground was assumed to be thermally insulated while a constant temperature equal to the initial temperature of the ground was considered for the other sides (15 °C). Please note that the slope of the ground changed each time with a change in the soil permeability or the groundwater velocity to induce the required hydraulic gradient in an unconfined condition. The input parameters used in this study are summarized in Table 1.

As indicated in Table 1, in this study, a uniform temperature of $15\,^{\circ}\mathrm{C}$ was considered as the initial temperature of the ground. It should be noted in real cases, the ground temperature increases with depth which influences the soil response to the external thermal loading [2,36]. However, considering the relatively short length of the heat source and domain size in this study, compared to the general geothermal gradient of $0.02-0.03\,^{\circ}\mathrm{C/m}$ reported in the literature [39], the assumption of a uniform initial ground temperature remains valid. Furthermore, it should be added that this study specifically investigates the effect of

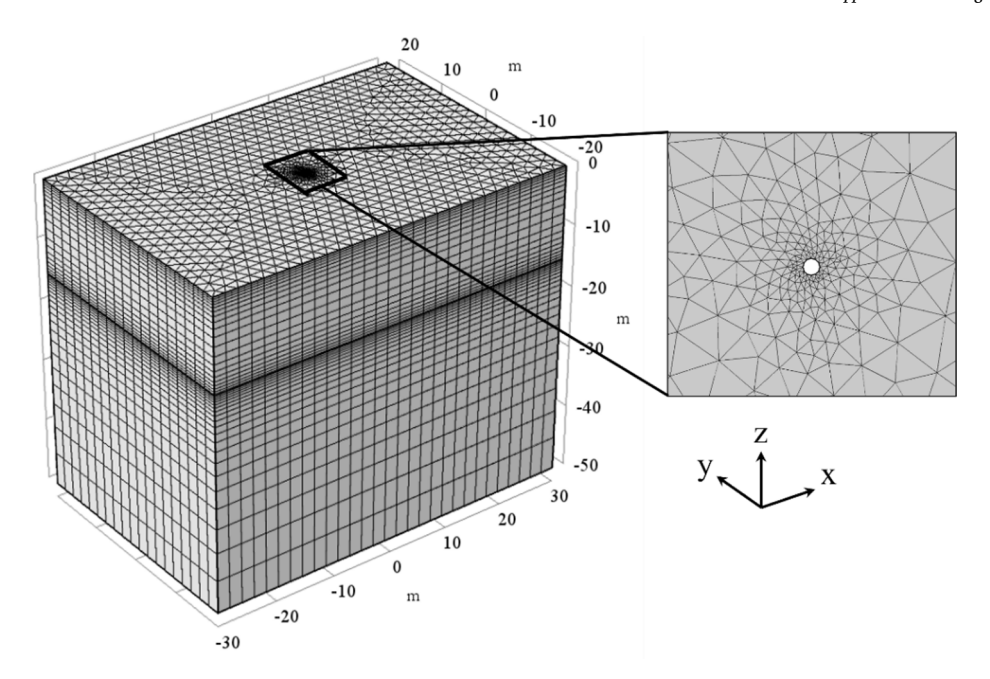


Fig. 2. Finite element mesh of the domain.

mixed convection on heat transfer within a homogeneous soil with uniform thermo-hydraulic properties. However, the thermo-hydraulic properties of the ground might change with depth affecting the amount of energy being transferred to the soil [8,39]. Therefore, further studies are needed to evaluate the effect of mixed convection in a heterogeneous layered ground.

Fig. 2 shows the finite element mesh used in the model. The surface was discretized using triangular elements with a finer mesh size close to the heat source. Subsequently, this 2D mesh configuration was extended along the depth to cover the entire 3D domain. As demonstrated, the distribution of the elements was more compact close to the surface and at the bottom of the heater to enhance the accuracy of the results. During the mesh sensitivity analysis, various mesh sizes were employed to examine the temperature change with depth and radial distance. Subsequently, the optimal mesh size and discretization were determined. It should be noted that this procedure was repeated for models with different heat source embedding depths.

2.2. Theory and governing equations

Soil hydro-thermal response was estimated by solving the mass, momentum, and energy balance equations simultaneously within the domain. Considering local thermal equilibrium between solid and fluid phases, the thermal energy balance equation, which takes into account the effect of conduction and fluid convection, can be expressed as:

$$(\rho C)_{m} \frac{\partial T}{\partial t} + (\rho C)_{f} u.\nabla T + \nabla \cdot (-k_{m} \nabla T) = 0$$
(1)

where ρ_m and ρ_f are respectively the medium and fluid density, C_m and C_f are specific heat capacity of the medium and fluid (i.e., groundwater), respectively, T represents the temperature, t shows the time, u is Darcy velocity, and k_m represents the thermal conductivity of the domain. It should be noted that, in this study, the effect of thermal dispersion on heat transfer has been neglected in order to focus on the influence of natural convection. However, considering the importance of thermal dispersion in high groundwater flow velocities, further studies are needed to explore the effect of thermal dispersion on hydro-thermal behavior of soils close to geothermal systems.

Heat capacity and thermal conductivity of the medium were calculated by considering the volumetric average of water and solid proper-

ties within the domain.

$$(\rho C)_m = (1 - \varphi)(\rho C)_s + \varphi(\rho C)_f \tag{2}$$

$$k_m = (1 - \varphi)k_s + \varphi k_f \tag{3}$$

where subscript s, and f represent solid and fluid phases, respectively, and φ denotes the porosity. Darcy velocity in Eq. (1) was obtained by solving mass and momentum balance equations for water, assuming that the fluid is incompressible, and porosity remains constant.

$$\varphi \frac{\partial \rho_f}{\partial t} + \nabla \cdot (\rho_f u) = 0 \tag{4}$$

$$u = -\frac{\kappa}{u} \nabla \cdot (p + \rho_f g z) \tag{5}$$

As mentioned earlier in the literature, natural convection occurs due to density gradient. In order to consider the density gradient in the analysis, the effect of temperature on density should be taken into account. Previous studies on the mixed convection effect on heat transfer have considered the Oberbeck-Boussinesq approximation to estimate the water density change with temperature [33,47]. However, this approximation is highly sensitive to the value of thermal expansion coefficient which is also a temperature-dependent parameter. To avoid inaccurate estimation of density, another relation by Hillel [26] was used to explore the effect of natural convection:

$$\rho_f = 1 - 7.37 \times 10^{-6} (T - 4)^2 + 3.79 \times 10^{-8} (T - 4)^3$$
 (6)

where T is temperature in $^{\circ}$ C.

The described partial differential equations were implemented in the developed finite element model in COMSOL Multiphysics software v5.3a. The solution was obtained through the backward differentiation formula (BDF) time-stepping method and using direct linear solvers (MUMPS and PARDISO). The relative tolerance of the time-dependent solver was set to 0.01 %.

2.3. Model validation

The presented finite element model was validated by simulation of an experiment conducted by Ghasemi-Fare and Basu [22] (for natural convection only), as well as a mixed convection problem studied by

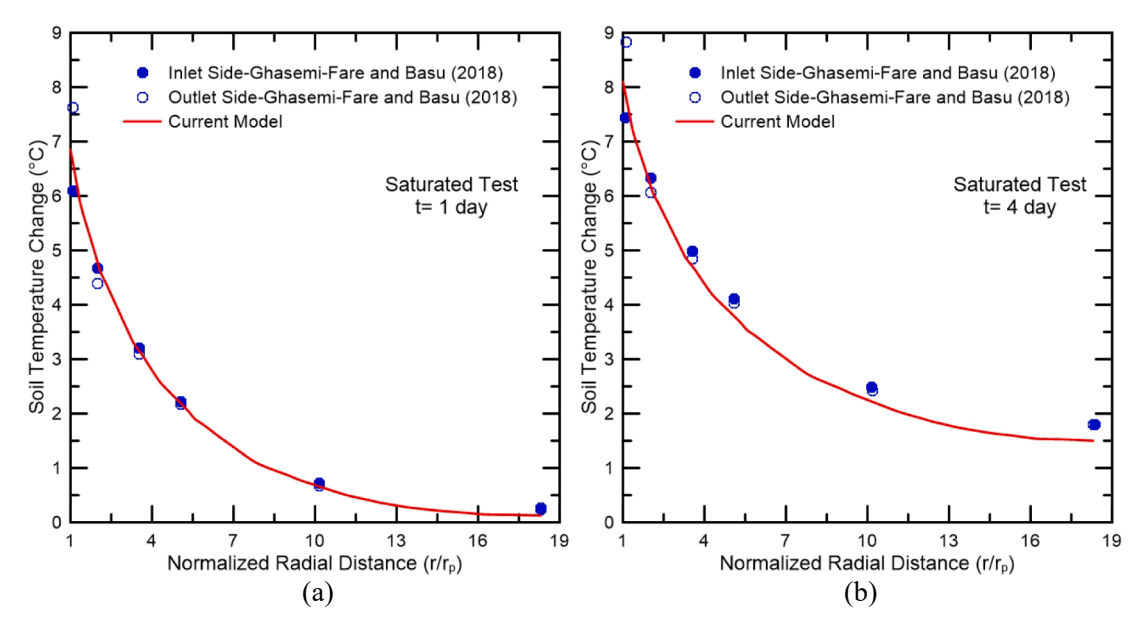


Fig. 3. Comparison of measured soil temperature increment during the experiment by Ghasemi-Fare and Basu [22] and predicted values using the developed FE model after a) 1 day, and b) 4 days.

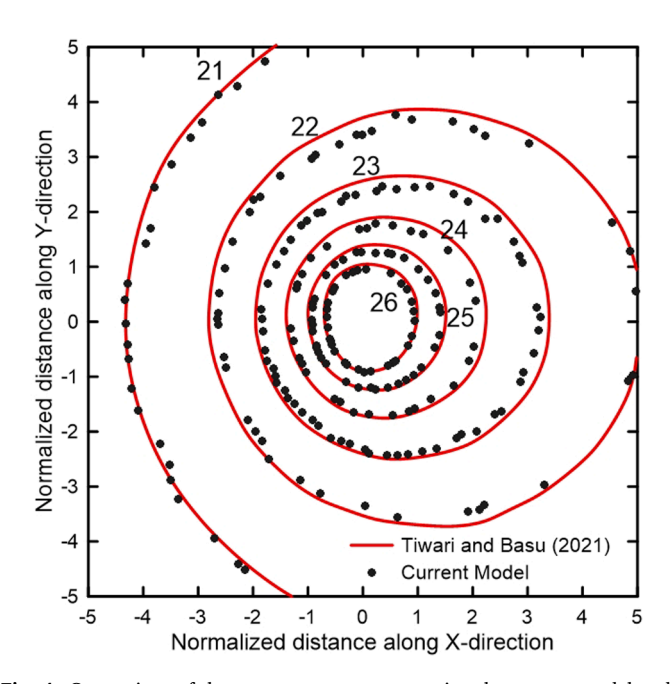


Fig. 4. Comparison of the temperature contours using the current model and those reported by Tiwari and Basu [47].

Tiwari and Basu [47]. Ghasemi-Fare and Basu [22] conducted a laboratory thermal performance test on a 1.38-m long model geothermal pile installed in a saturated soil (1.83 m \times 1.83 m \times 1.73 m). In their experiment, a heat carrier fluid with an inlet temperature of 41 °C was circulated inside a U-shaped tube. The soil temperature was measured throughout the tests using embedded thermocouples in different locations. The soil temperature increment reported by Ghasemi-Fare and Basu [22] after 1 day and 4 days were compared to the numerical results obtained from the developed FE model (Fig. 3). As demonstrated, the FE results are in good agreement with the measured data during the experiment. Comparing the experimental and numerical results, the FE model estimated the soil temperature change after 1 day and 4 days of heating with a Root Mean Square Error (RMSE) of 0.36 and 0.39 °C, respectively. Details of the experiment and adopted parameters as well

as additional equations for considering heat transfer through the pipe are presented in Appendix A.

Tiwari and Basu [47] numerically explored the influence of mixed convection on the effective thermal conductivity of a saturated medium. To do so, they analyzed the soil temperature near a geothermal pile with a diameter of 0.15 m and a length of 60 m. The analysis was taken in a ground that was saturated with a permeability of 5×10^{-9} m² and subjected to a groundwater flow with a velocity of 10^{-6} m/s. Other required parameters including the soil, pipe, and fluid properties are adopted from Tiwari and Basu [47]. Fig. 4 shows the temperature contours after 7 days (168 h) of heating with a heat rate of 60 W/m (temperature is reported in °C). A comparison of temperature contours obtained from the current model and those from the study by Tiwari and Basu [47] revealed an RMSE of 0.20 °C. As demonstrated, the results of the current model are consistent with the data reported by Tiwari and Basu [47]. Please see Appendix A for more information regarding problem geometry and input parameters.

3. Results and discussion

3.1. Natural convection effect

In order to investigate the influence of natural convection on soil hydro-thermal response close to an embedded heat source in a saturated porous medium in the presence of an unconfined groundwater flow (forced convection), a parametric study was performed using the FE model as described above. Different permeabilities $(10^{-9},\,10^{-10},\,10^{-11},\,$ and $10^{-12}\,\mathrm{m}^2)$ and groundwater flow velocities $(10^{-6},\,5\times10^{-7},\,10^{-7},\,10^{-8}$ and $10^{-9}\,\mathrm{m/s})$ were considered in the model to assess the significance of natural convection under various conditions. Furthermore, various heat source temperatures (40, 60, and 80 °C) were implemented in the model to represent different practical applications from geothermal heat exchangers installed to heat and cool residential buildings that have lower temperature variations to geothermal energy storage systems which are of higher temperature.

Fig. 5 shows the thermal response of the soil along a line parallel to the surface passing through the mid-depth of the pile after 1000 days (when soil temperature close to the heat source reaches nearly a steady state condition). The temperature of the heat source was kept at a constant temperature, 80 $^{\circ}$ C, throughout the analysis. Please note that due to the large number of scenarios (60 in total), only a part of the

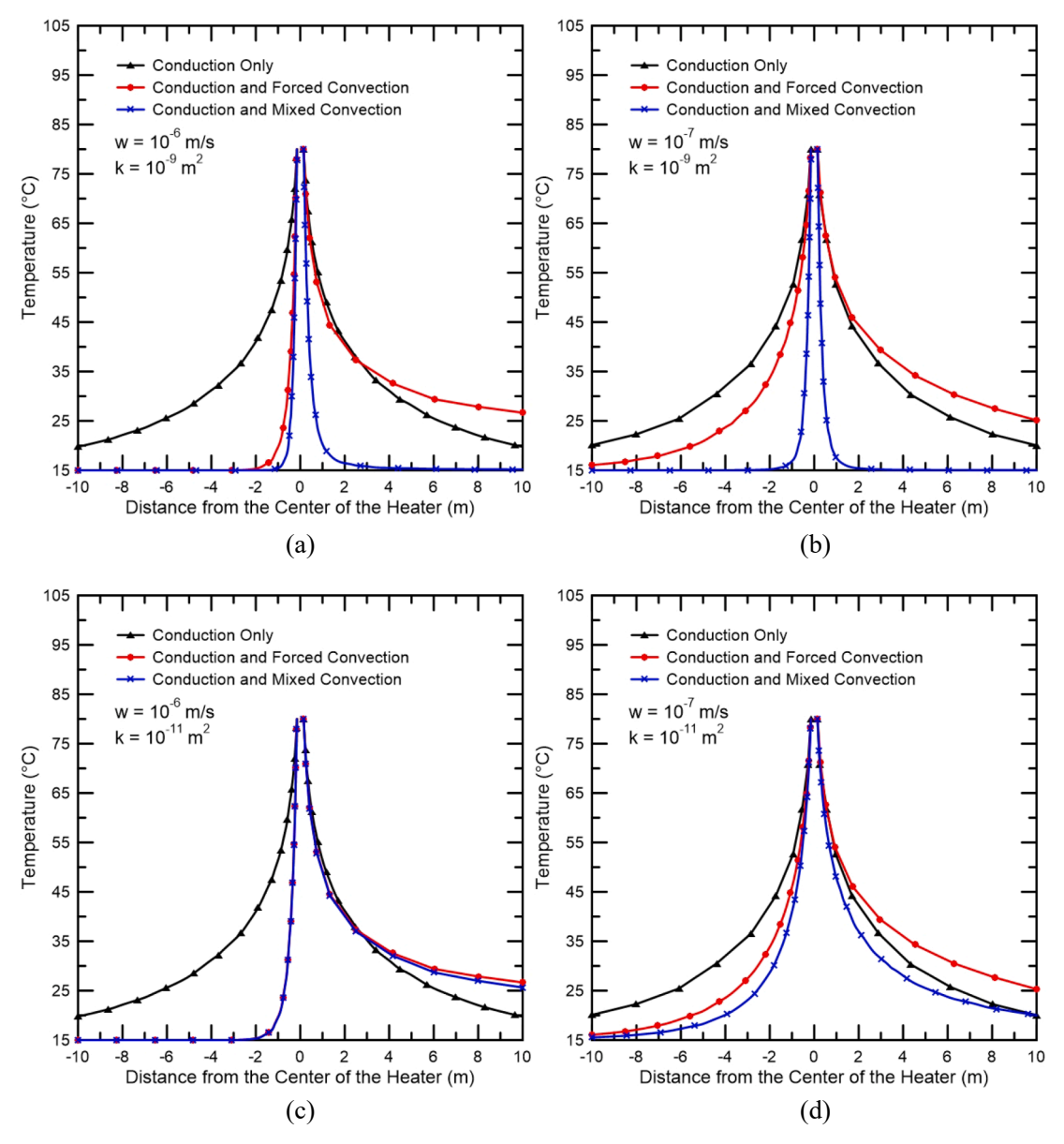


Fig. 5. Temperature distribution close to a heat source with $T_h = 80$ °C considering different heat transfer mechanisms when a) $w = 10^{-6}$ m/s, $\kappa = 10^{-9}$ m², b) $w = 10^{-7}$ m/s, $\kappa = 10^{-9}$ m², c) $w = 10^{-6}$ m/s, $\kappa = 10^{-11}$ m², and d) $w = 10^{-7}$ m/s, $\kappa = 10^{-11}$ m².

results are shown in this figure. As demonstrated in Fig. 5a, at the condition with $w = 10^{-6}$ m/s and $\kappa = 10^{-9}$ m², the thermal response of the soil on the inlet side under mixed convection is almost similar to that observed when only forced convection was considered. However, under mixed convection, the soil temperature on the outlet side (right side of the heat source) is significantly lower compared to the results obtained from a forced convection condition (when natural convection is neglected). To better explain the reason behind this phenomenon, temperature contours, and fluid velocity vectors are shown in Fig. 6a. As illustrated, natural convection directs the water toward the heat source due to the density gradient in the heated zone. Given the groundwater flow direction, the effect of natural and forced convection on temperature distribution in the inlet would be the same. The combined effect of forced and natural convection resulted in a small drop in soil temperature close to the heater on the inlet side when natural convection was considered. Nevertheless, on the outlet side, natural and forced convection flow in opposite directions, and considering the magnitude of fluid velocity and thermal gradient, natural convection dominates the forced convection close to the heat source. This dominance prohibits

heat propagation to farther distances on the outlet side. Consequently, lower soil temperature was observed when natural convection was taken into account.

When the groundwater flow velocity decreased to 10^{-7} m/s (Fig. 5b) while keeping the soil permeability constant ($\kappa = 10^{-9} \text{ m}^2$), the difference between soil temperature obtained from forced and mixed convection on the inlet side intensified. This happened because, at the lower groundwater flow, heat convection mechanism under natural convection was more significant than that of forced convection (Fig. 6b). Conversely, when the soil permeability was reduced to 10^{-11} m² (as shown in Fig. 5c) while maintaining the same groundwater flow velocity $(w = 10^{-6} \text{ m/s})$, the disparity between the temperature distribution obtained from mixed and forced convection diminished completely. This happened because of the small natural convection velocity and thus a lower ratio of natural convection velocity over groundwater velocity, which is a result of the low permeability (Fig. 6c). However, at the same permeability of 10^{-11} m², when the groundwater velocity reduced to 10^{-7} m/s (Fig. 5d), that difference between mixed and forced convection started to appear again, because of the larger value for natural

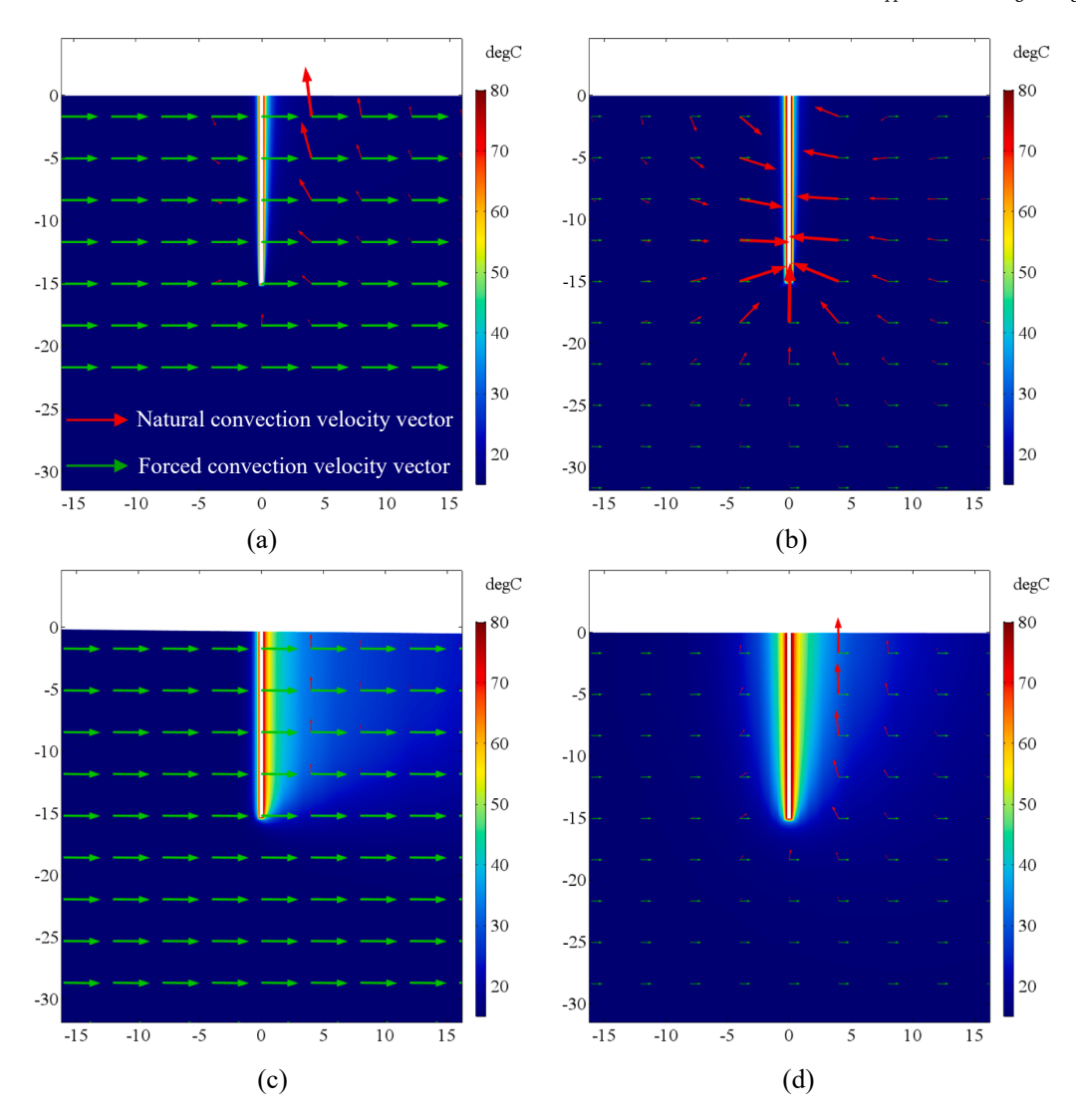


Fig. 6. Soil temperature contours, natural and forced convection velocity vectors adjacent to the heat source with a temperature of 80 °C when a) $w = 10^{-6}$ m/s, $\kappa = 10^{-9}$ m², b) $w = 10^{-7}$ m/s, $\kappa = 10^{-9}$ m², c) $w = 10^{-6}$ m/s, $\kappa = 10^{-11}$ m², and d) $w = 10^{-7}$ m/s, $\kappa = 10^{-11}$ m².

convection velocity compared to that of forced convection (Fig. 6d).

Fig. 5 also shows the results of the analysis when conduction was considered as the sole heat transfer mechanism. It is obvious that in all cases, forced convection led to a decrease in temperature on the inlet side while it increased the soil temperature on the outlet side. Indeed, soil temperature was increased in the direction of the groundwater flow. However, at a lower groundwater flow velocity, the difference between the results obtained from forced convection and conduction-only analysis was decreased. Therefore, it can be deduced that in the case of low groundwater velocity, there is no necessity to consider forced convection in heat transfer analysis. On the other hand, as demonstrated in Fig. 5b, despite the reduction in groundwater flow rate (compared to Fig. 5a), there is still a considerable difference between the soil temperature obtained from conduction-only and mixed convection models. This finding suggests that natural convection still plays a vital role in this range of groundwater velocity.

As demonstrated, the natural convection role in heat transfer varies with changes in the soil permeability and groundwater flow velocity. To quantitatively determine the importance of natural convection in heat transfer analysis, the average temperature difference between forced and mixed convection, for 100 equally spaced points on the line passing the mid-depth of the heater, was calculated, and normalized based on the initial temperature difference between the ground and the heater.

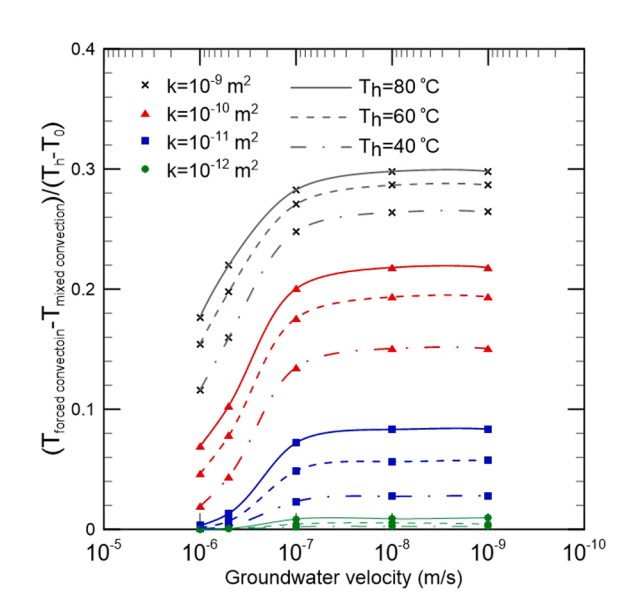


Fig. 7. Variation of difference between forced and mixed convection results with groundwater velocity change.

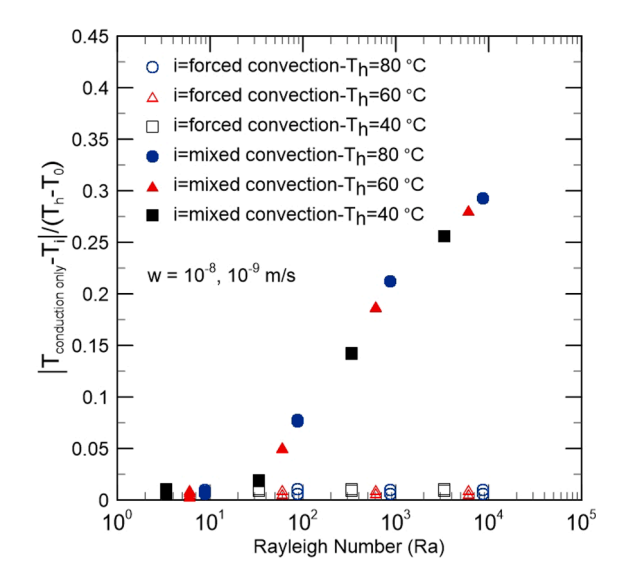


Fig. 8. Variation of the normalized temperature difference between forced convection and conduction, and that of mixed convection and conduction with Rayleigh number variation when $w < 10^{-7}$ m/s.

This procedure was repeated for all different scenarios explored in this study (all 60 cases). Fig. 7 shows the variations of normalized temperature difference with respect to changes in subsurface flow velocity. As demonstrated, the normalized temperature difference increased with a decrease in groundwater flow velocity for all heater temperatures and soil permeabilities. Nonetheless, for groundwater velocities below 10^{-7} m/s, the normalized temperature difference remained constant despite alterations in groundwater velocity. This can be interpreted as when the groundwater flow velocity reduces to a value lower than 10^{-7} m/s, the influence of forced convection on heat transfer is negligible in comparison to other mechanisms. This is consistent with the findings of previous studies in the literature, suggesting that the contribution of forced convection in heat transfer might be trivial in scenarios with w < 10^{-7} m/s [4,13,35]. Nevertheless, the role of natural convection in heat transfer within this range of groundwater flow velocity (e.g., lower than 10^{-7} m/s) should be evaluated.

Given the fact that heat source temperature and soil permeability are still affecting the normalized temperature difference in this range of groundwater velocity (less than 10^{-7} m/s), Rayleigh number (Ra) was calculated for the scenarios with the groundwater flow velocities of 10^{-8} and 10^{-9} m/s using Eq. (7). The Rayleigh number considers the influence of permeability and heater temperature.

$$Ra = \frac{g\beta\kappa L_h\Delta T}{L_{col}} \tag{7}$$

where β is the volumetric thermal expansion coefficient, L_h is the heater length, ν is the kinematic viscosity of water, and α is the thermal diffusivity of the medium. It should be mentioned that in order to obtain a single Ra number for each scenario, ΔT was assumed to be the difference between the heater and initial soil temperature. Fig. 8 shows the normalized temperature difference between forced convection and conduction, as well as that of mixed convection and conduction versus Ra number for groundwater flow velocities of $w = 10^{-8}$ and 10^{-9} m/s. As illustrated, in this range of groundwater flow velocity, forced convection does not play any considerable role in heat transfer, and normalized temperature differences between forced convection and conduction results are negligible. Adopting a threshold of 5 % or higher for significant changes in normalized temperature, it was found that for a Ra greater than 50, the difference between mixed convection and conduction temperature is significant. Therefore, it can be concluded that for a groundwater flow velocity less than 10^{-7} m/s (which was determined from Fig. 7), natural convection should be taken into

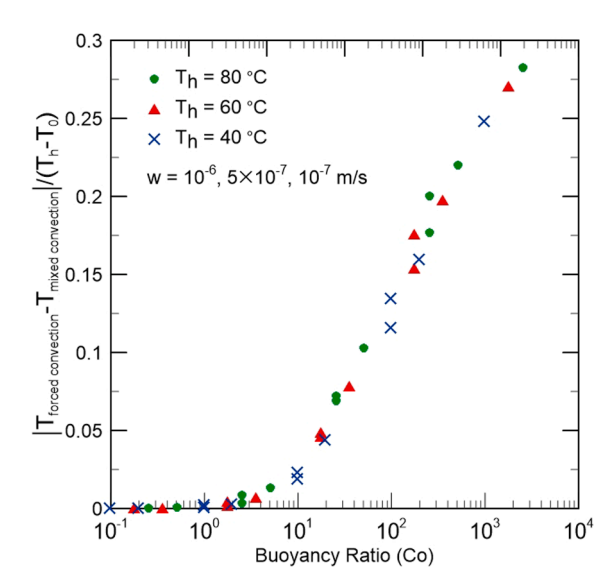


Fig. 9. Variation of the normalized temperature difference between forced and mixed convection with buoyancy ratio change when $w > 10^{-7}$ m/s.

account only when Ra is greater than 50. This threshold is in good agreement with the critical Ra number defined in the literature for the saturated porous media which is subjected to a thermal gradient from the bottom boundary. According to that, natural convection role in heat transfer in an infinitely extensive horizontal layer, under the no-forced convection condition, is non-negligible when Ra number is larger than $4\pi^2$ [3.29.30].

As demonstrated in Fig. 7, when the groundwater flow velocity is equal to or greater than 10^{-7} m/s, in addition to heater temperature and soil permeability, groundwater flow velocity should also be considered in the heat transfer analysis. In this regard, another non-dimensional number named buoyancy ratio or mixed convection number (*Co*) [27,28,29], which is the ratio of Rayleigh to Peclet number, was calculated following Eq. (8) for the scenarios with a groundwater velocity greater or equal to 10^{-7} m/s.

$$Co = \frac{Ra}{Pe} = \frac{\beta \Delta T}{i} \tag{8}$$

where $Pe=wL_h/\alpha$ denotes the Peclet number, and i is the hydraulic gradient. Fig. 9 shows the normalized temperature difference between considering natural convection (mixed convection) and not considering that (forced convection only) in heat transfer analysis. As illustrated, with an increase of Co number, the difference between mixed and forced convection increases. The higher difference between natural convection and forced convection determines the stronger role of natural convection in heat transfer. Please note that an increase in Co number represents an increase in the soil permeability or heat source temperature, or a decrease in groundwater velocity, which all enhances the role of natural convection over forced convection. Considering the same 5 % change as the threshold, it can be stated that for a $Co \geq 20$, natural convection should be considered in heat transfer analysis.

In order to summarize the conclusion and provide recommendations on considering natural convection under both hydrostatic and hydrodynamic conditions, a flow chart containing both Ra and Co numbers is provided in Fig. 10. As illustrated, depending on the groundwater flow velocity, Ra, and Co number, different mechanisms might play significant roles in heat transfer within a saturated porous medium. Considering this flowchart, by knowing the groundwater velocity, soil permeability, and heat source temperature, the dominant heat transfer mechanisms are suggested. Using the suggested mechanisms, soil thermal response can be determined more accurately while reducing unnecessary computational costs.

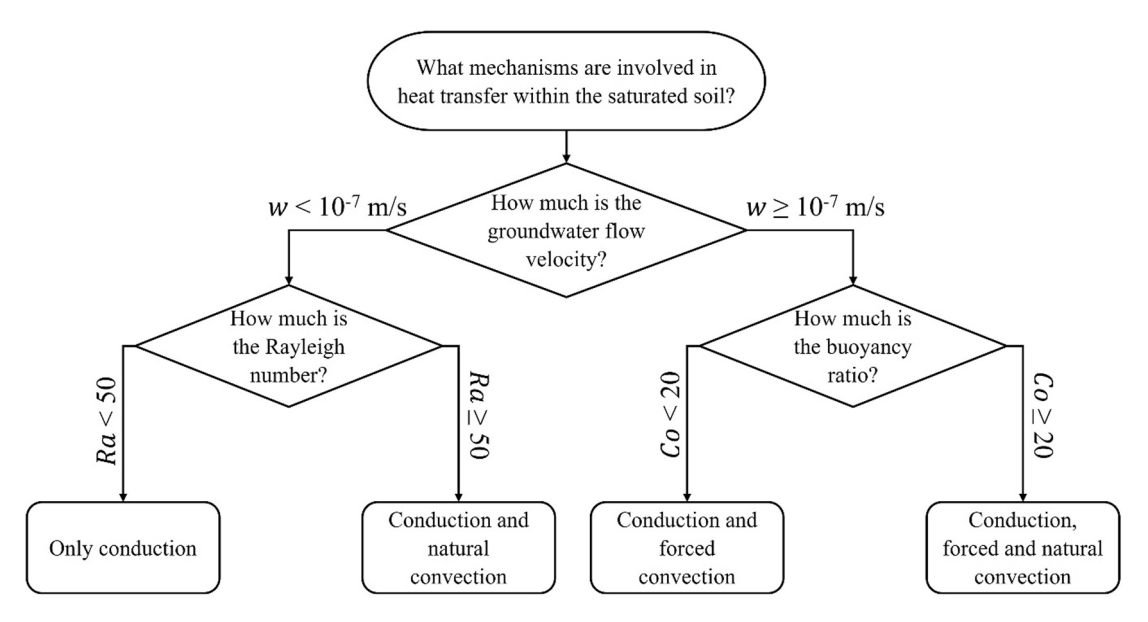


Fig. 10. Flowchart showing the heat transfer mechanisms in different conditions.

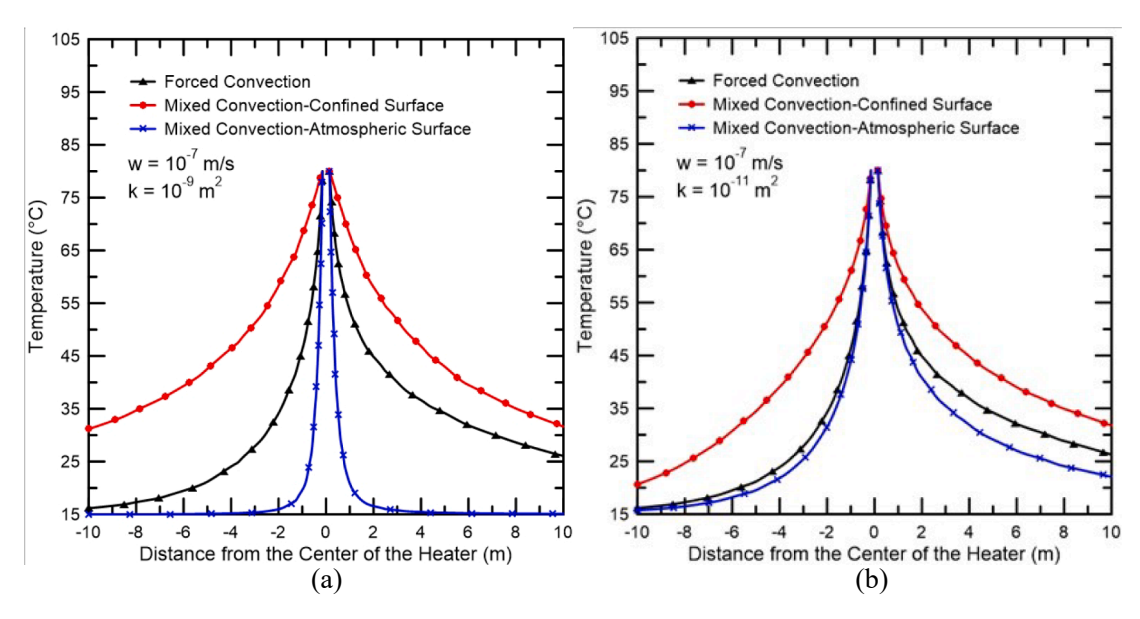


Fig. 11. Soil temperature distribution at the surface with and without considering the natural convection under different boundary conditions in a medium with a) $\kappa = 10^{-9} \text{ m}^2$ and b) $\kappa = 10^{-11} \text{ m}^2$.

3.2. Hydraulic boundary condition effect

As mentioned in the introduction, previous studies that assessed the coupled effect of natural and forced convection on heat transfer in a soil medium assumed a confined boundary condition at the ground surface. This assumption results in different pressures at the surface compared to the atmospheric pressure. To highlight the role of surface boundary conditions on natural convection influence on heat transfer, a confined boundary condition was considered for the surface in the developed FE model, and the results were compared to the results of the unconfined model that was presented in the previous section.

Fig. 11 shows the soil temperature distribution at the ground surface considering different boundary conditions when $T_h=80\,^{\circ}\text{C}$, and $w=10^{-7}\,\text{m/s}$. As demonstrated in Fig. 11a, in a confined boundary condition with a permeability of $10^{-9}\,\text{m}^2$, mixed convection resulted in higher temperatures compared to forced convection alone, while an opposite trend was observed under the unconfined boundary condition. In other

words, when the confined boundary condition was applied to the surface, natural convection caused an increase in temperature at the surface, whereas the unconfined boundary condition resulted in a reduction of temperature due to natural convection. This behavior is attributed to the direction of natural convection flow (Fig. 12). As illustrated, the natural convection flow occurred towards both the heat source and the surface. However, in the presence of a confined boundary condition, the direction of natural convection flow changed, and became predominantly horizontal in the close proximity of the surface (Fig. 12a). Therefore, thermal energy transferred by natural convection was distributed along the surface, resulting in an increase in the surface temperature. Nevertheless, the unconfined boundary condition did not change the direction of the natural convection flow and therefore the thermal energy was kept close to the heat source (Fig. 12b).

As illustrated in Fig. 11b, with a decrease in the soil permeability, the difference between forced and mixed convection results is reduced in the unconfined condition. This behavior is related to a lower natural

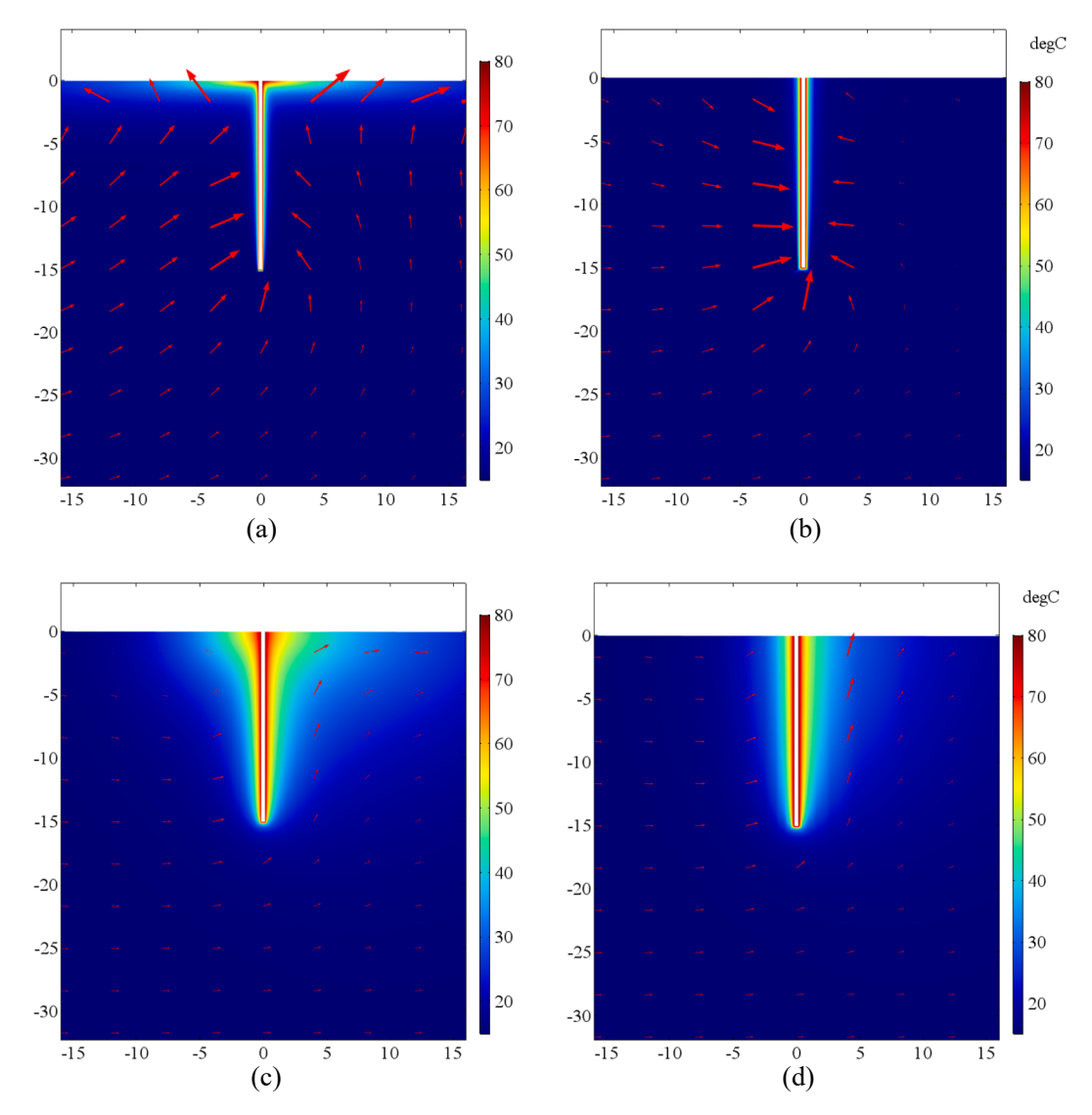


Fig. 12. Comparison of soil temperature contours and mixed convection flow velocity vectors under the influence of confined (a and c) and unconfined (b and d) boundary conditions in the presence of groundwater flow with $w = 10^{-7}$ m/s when a-b) $\kappa = 10^{-9}$ m² and c-d) $\kappa = 10^{-11}$ m².

convection velocity magnitude at this permeability (Fig. 12d). However, as demonstrated in Fig. 12c, in the confined boundary condition, the x component of fluid velocity close to the surface (especially after the heat source) was still larger than that of forced convection (see the fluid velocity vectors below the heat source as a representative of forced convection flow magnitude). As a result, the difference between forced and mixed convection temperature distribution was still considerable in the confined condition (Fig. 11b) at the lower permeability.

As mentioned in the introduction, previous studies that investigated the effect of mixed convection on heat transfer, did not consider the effect of boundary conditions in their analyses and just assessed that matter in a confined condition. However, as mentioned before, this assumption is not always correct. On the other hand, according to the results of this section, fluid velocity direction and magnitude are highly dependent on the surface boundary condition, which consequently affect the role of mixed convection in heat transfer. To highlight the effect of surface hydraulic boundary condition on thermal energy distribution, the Mean Absolute Percentage Error (MAPE) was calculated for 100 equally spaced points, which were selected on the lines shown in Fig. 11, while the unconfined boundary condition (atmospheric surface) was taken as the reference. By comparing the temperature distributions of confined and unconfined conditions, an MAPE of 173 % was obtained

for the case with a groundwater flow velocity of 10^{-7} m/s and a permeability of 10^{-9} m². However, with a reduction of permeability to 10^{-11} m² at the same groundwater flow velocity, the MAPE was reduced to 47 %. Accordingly, it can be concluded that the role of mixed convection and its effect on heat transfer highly depends on the hydraulic boundary condition, and assuming an incorrect boundary condition can substantially affect the results.

It should be mentioned that in a preliminary analysis, instead of a thermally insulated boundary condition, a convective boundary was considered for the unconfined surface to simulate a more realistic case (not shown here). Although the soil temperature on the surface was different than the thermally insulated condition, the effect of natural convection on reducing the soil temperature was the same. Therefore, as the main purpose of this study was to evaluate the effect of hydraulic boundary conditions (confined versus unconfined), a similar thermal boundary (thermal insulation) was employed in our analyses for both confined and unconfined boundary conditions. Nevertheless, further studies are needed to evaluate the role of natural convection on soil hydro-thermal response in a more complex thermal boundary condition, which can take the effects of air temperature fluctuations, wind speed, solar radiation, etc. into account.

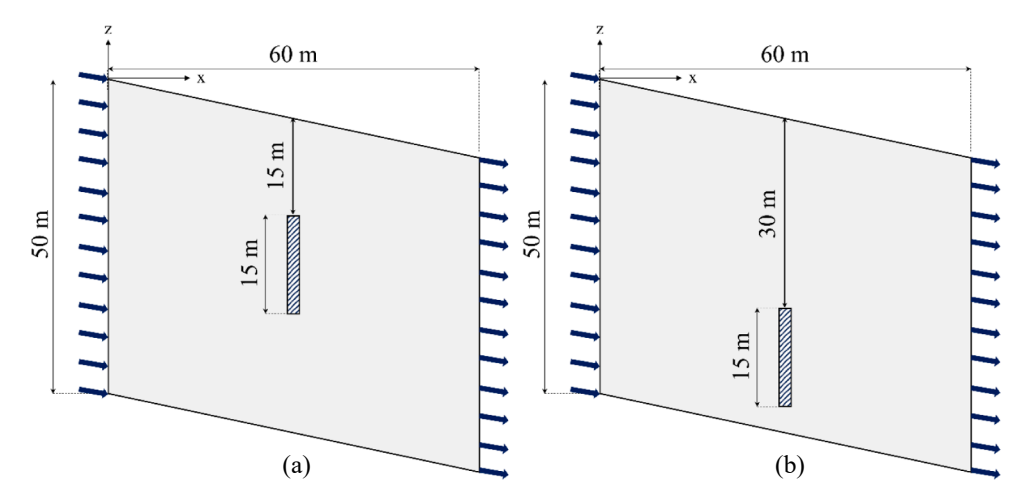


Fig. 13. Schematic of the models with the heat source being embedded at a depth of a) 15 m and b) 30 m.

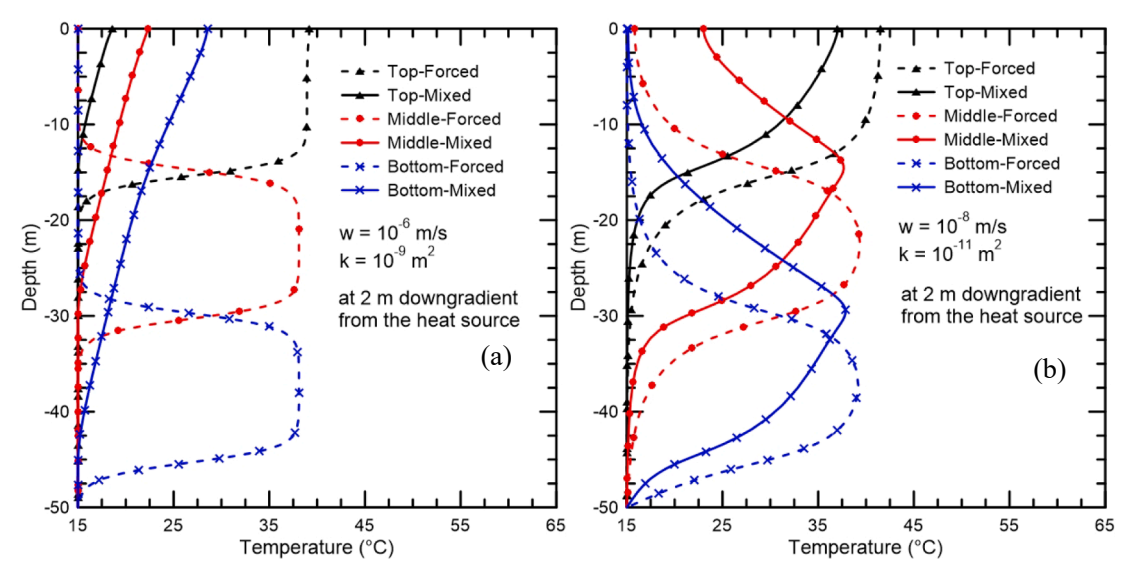


Fig. 14. Soil temperature variation with depth at 2 m downgradient of the heat source while locating the heat source at different depths when a) $w = 10^{-6}$ m/s, $\kappa = 10^{-9}$ m², and b) $w = 10^{-8}$ m/s, $\kappa = 10^{-11}$ m².

3.3. Heat source location effect

This paper also investigated the effect of heat source location on the soil hydro-thermal response to assess if natural convection plays different roles when the heat source is embedded at varying depths. In this regard, in addition to the previous model in which the heater was located at the top part of the model, different embedding depths of 15 and 30 m were considered for the heat source in the developed FE model (Fig. 13).

Fig. 14 shows the soil temperature profile at 2 m downgradient from the heat source ($T_h=80\,^{\circ}\text{C}$). In the case with $\kappa=10^{-9}$ m² and $w=10^{-6}$ m/s (Fig. 14a), natural convection lowered the soil temperature significantly compared to forced convection when the heat source was located at the top. However, when the heater was positioned in the middle or bottom of the domain, the vertical movement of buoyant flow led to an increase in temperature above the heater, and therefore mixed convection resulted in higher soil temperatures above the heater compared to forced convection. Furthermore, it was observed that for the same conditions ($\kappa=10^{-9}$ m² and $w=10^{-6}$ m/s) and at this particular distance from the heater (2 m downgradient from the heater which is reported in Fig. 14), the surface temperature was highest when the heater was located at the bottom. However, altering the groundwater flow and

permeability (Fig. 14b) resulted in a distinct temperature profile. With a decrease in permeability, the role of natural convection in heat transfer diminished, leading to a reduction in the temperature difference between mixed and forced convection. Nevertheless, still, when the natural convection was considered in the models with the heater being located at the middle or bottom of the domain, the peak temperature occurred above the heater. This is attributed to the mixed convection flow towards the surface which resulted in redistribution of the thermal energy towards shallower depths (see Fig. 15). However, as demonstrated in Fig. 15, at depths farther from the heat source, the magnitude of mixed convection velocity and hence the temperature was lowered in this soil permeability ($\kappa=10^{-11}\ m^2$).

To better evaluate the effect of natural convection on heat transfer when the heat source is embedded in different depths, the MAPE was calculated for cases shown in Fig. 14. Based on the results, in the scenario with a groundwater flow velocity of 10^{-6} m/s and a permeability of 10^{-9} m², neglecting the natural convection resulted in MAPEs of 43, 48, and 60 % when the heat source was embedded in the top, middle, and bottom, respectively. However, in the case with a groundwater flow velocity of 10^{-8} m/s and permeability of 10^{-11} m², the MAPE value reduced to 13 % for the top-embedded heater, 22 % for the one in the middle, and 21 % for the one in the bottom. Accordingly, it can be

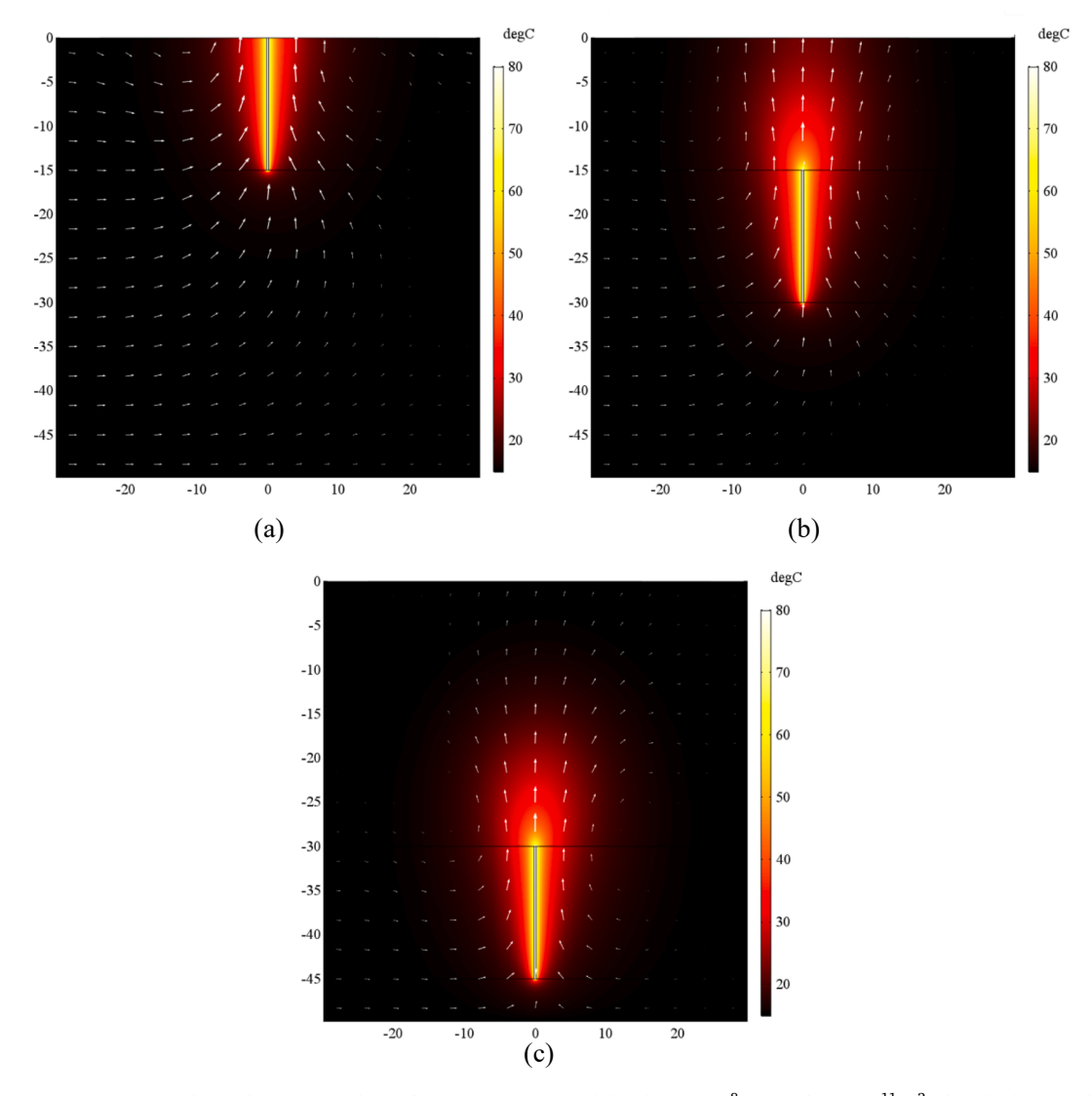


Fig. 15. Soil temperature contours and mixed convection flow velocity vectors in a model with $w = 10^{-8}$ m/s and $\kappa = 10^{-11}$ m² when the heater is located at a) top, b) middle, and c) bottom of the domain.

concluded that with an increase in the embedding depth, the effect of natural convection on heat transfer, and hence on soil temperature distribution intensifies.

It is important to note that the dominant heat transfer mechanism varies at different distances from the heater, depending on the soil permeability and groundwater flow velocity. As a result, the general distribution of the soil temperature profile may change at different distances. For instance, the soil temperature profile at locations very close to the heat source (e.g., 0.05 m away from the heat source), is different than what has been reported at a distance of 2 m away from the heat source. In close proximity to the heater, the magnitude of fluid velocity reduces due to the no-flow boundary condition of the heater. Consequently, the role of conduction is more significant compared to the forced and natural convection in this very close vicinity to the heat source. Therefore, in such cases, when the heat sources are located at the middle or bottom, they mainly contribute to increasing the temperature in the surrounding area in a radial manner rather than having a significant effect on the soil temperature near the surface.

4. Conclusion

This paper identifies the importance of natural convection in the heat transfer mechanism close to an embedded heat source in a saturated ground with a subsurface flow. Heat transfer was numerically analyzed through a 3D finite element model that was developed in COMSOL Multiphysics, which considers the coupled effect of natural and forced convection in the governing hydro-thermal equations. Unlike previous studies, in this study, natural convection effect was scrutinized in the presence of an unconfined groundwater flow instead of a confined subsurface flow, using an inclined geometry. A parametric study was conducted to assess the role of natural convection in different scenarios. The effect of natural convection in heat transfer was quantitatively related to two non-dimensional numbers (Ra and Co) which take into account the effect of soil permeability, groundwater velocity, and heat source temperature. The results suggest that for the cases in which the groundwater velocity is less than 10^{-7} m/s, there is no need to consider forced convection in analysis, while natural convection should only be considered when $Ra \ge 50$. Moreover, in cases where groundwater velocity is equal to or greater than 10^{-7} m/s, natural convection plays a significant role in heat transfer only when Co > 20. Furthermore, the role of natural convection under confined and unconfined surface boundary conditions was examined. It was revealed that relative to the forced convection results, natural convection led to an increase in the soil temperature at the surface under a confined boundary condition, while it reduced the soil temperature at the surface under an unconfined condition. Additionally, assuming a confined boundary condition for the

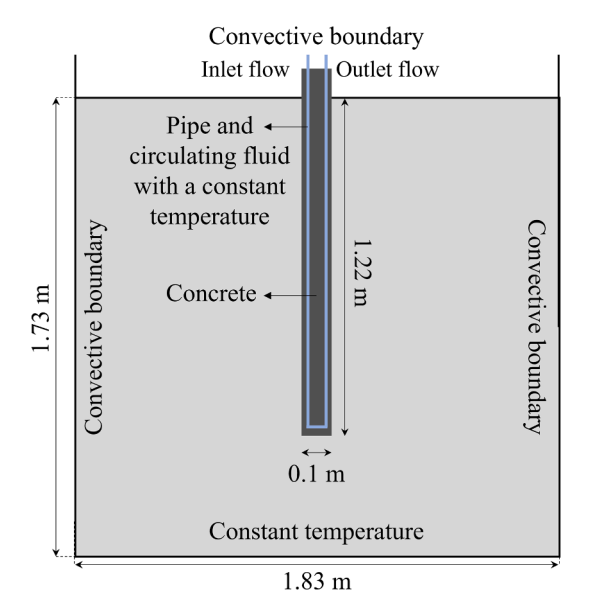


Fig. A1. Schematic of a thermal performance test conducted by Ghasemi-Fare and Basu [22].

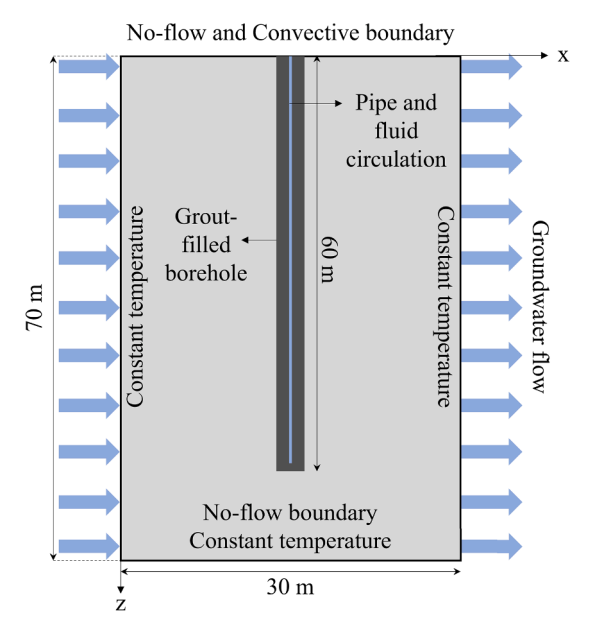


Fig. A2. Schematic of the mixed convection problem analyzed by Tiwari and Basu [47].

surface instead of an unconfined one resulted in 47 to 173 % error in the soil temperature distribution for the investigated scenarios. Finally, by analyzing the heat transfer in scenarios with varying heat source locations relative to the ground surface, it was found that the effect of natural convection is more significant in the cases where heat source is located farther from the surface (errors of 43, 48, and 60 % in the soil temperature distribution at a 2-m distance downgradient from the heater for the heat source inserted at top, middle and bottom when $\kappa=10^{-9}~\text{m}^2$ and $w=10^{-6}~\text{m/s}$). It was also demonstrated that natural convection flows toward the surface, facilitating the thermal energy transfer to the area above the heater, and thus highest soil temperature appeared above the heat source. However, the extent to which thermal energy is transferred to the areas above the heater depends on the soil permeability and the groundwater flow velocity.

Table A1

Model input parameters reported by Ghasemi-Fare and Basu [22].

Parameter	Value
Convective heat transfer coefficient (hg)	$0.02 \text{ W/m}^2/\text{K}$
Initial ground temperature (T ₀)	21 °C
Circulating fluid inlet temperature (Tin)	41 °C
Fluid circulation velocity (u _{cf})	0.66 m/s
Pile Diameter (D _p)	0.1 m
Pile length (L _p)	1.22 m
Circulation tube radius (r _t)	0.006 m
Shank distance (s _t)	0.02 m
Density of the heat carrying fluid (ρ _{cf})	1060 kg/m^3
Dynamic viscosity of the heat carrying fluid (μ_{cf})	$2.2 imes 10^{-3}$ Pa s
Specific heat capacity of the heat carrying fluid (Ccf)	3455 J/kg/K
Thermal diffusivity of the concrete (α _c)	$4.8 \times 10^{-7} \text{ m}^2/\text{s}$
Thermal diffusivity of the saturated soil ($\alpha_{s, sat}$)	$7.6 \times 10^{-7} \text{m}^2/\text{s}$
Thermal conductivity of the heat carrying fluid (kcf)	0.41 W/m/K
Thermal conductivity of the concrete (k _c)	1.5 W/m/K
Thermal conductivity of the saturated soil $(k_{s, sat})$	3.2 W/m/K

Table A2Model input parameters reported by Tiwari and Basu [47].

Parameter	Value
Convective heat transfer coefficient (hg)	1 W/m ² /K
Initial ground temperature (T ₀)	20 °C
Heat rate (q _h)	60 W/m
Fluid circulation flow velocity (u _{cf})	0.31 m/s
Borehole diameter (Db)	0.15 m
Circulating tube inner radius (r _{t, in})	0.0125 m
Circulating tube outer radius (r _{t, out})	0.0148 m
Shank distance (s _t)	0.1 m
Porosity (φ)	$0.41 \text{ m}^3/\text{m}^3$
Permeability (κ)	$5\times 10^{-9}\ m^2$
Density of the heat carrying fluid (ρ _{cf})	1000 kg/m^3
Density of the borehole grout (ρ_b)	1500 kg/m^3
Dynamic viscosity of the heat carrying fluid (μ_{cf})	$0.862 \times 10^{-3} \mathrm{Pa} \mathrm{s}$
Specific heat capacity of the circulation tube (Ct)	2000 J/kg/K
Specific heat capacity of the heat carrying fluid (Ccf)	4190 J/kg/K
Specific heat capacity of the borehole grout (Cb)	1500 J/kg/K
Specific heat capacity of the ground (Cg)	800 J/kg/K
Thermal conductivity of the circulation tube (k _t)	0.4 W/m/ K
Thermal conductivity of the heat carrying fluid (k _{cf})	0.6 W/m/K
Thermal conductivity of the borehole grout (k _b)	1.6 W/m/K
Thermal conductivity of the ground (kg)	2.9 W/m/K

CRediT authorship contribution statement

Fereydoun Najafian Jazi: Resources, Conceptualization, Methodology, Software, Formal analysis, Investigation, Data curation, Writing – original draft, Writing – review & editing. Omid Ghasemi-Fare: Project administration, Conceptualization, Methodology, Supervision, Data curation, Funding acquisition, Writing – original draft, Writing – review & editing. Thomas D. Rockaway: Project administration, Conceptualization, Methodology, Supervision, Data curation, Funding acquisition, Writing – review & editing.

Declaration of Competing Interest

The authors declare that they have no known competing financial interests or personal relationships that could have appeared to influence the work reported in this paper.

Data availability

Data will be made available on request.

Acknowledgment

The authors would also like to gratefully acknowledge the financial

support by the National Science Foundation under Grant No. CMMI- 1804822.

Appendix A

The geometry of the experiment conducted by Ghasemi-Fare and Basu [22] and the mixed convection problem simulated by Tiwari and Basu [47] are illustrated in Figs. A.1 and A.2, respectively. Moreover, the corresponding input parameters for modeling these problems are presented respectively in Table A.1 and A.2.

It needs to be noted that in these problems, to simulate heat transfer by the heat carrying fluid inside the pipe, additional equations were needed to be considered. In this regard, the energy equation for the heat carrying fluid was implemented in the described FE model as follows:

$$\rho_{cf}C_{cf}\frac{\partial T_{cf}}{\partial t} + \rho_{cf}C_{cf}u_{cf} \cdot \nabla T_{cf} - \nabla (k_{cf}\nabla T_{cf}) - \frac{1}{4}f_{D}\frac{\rho_{cf}}{r_{tin}}|u_{cf}|u_{cf}^{2} = \frac{q_{wall}}{A_{t}}$$
(A.1)

where ρ_{cf} , C_{cf} , T_{cf} , u_{cf} , and k_{cf} are density, specific heat capacity, temperature, velocity, and thermal conductivity of the heat carrying fluid, respectively. $r_{t.in}$ and A_t are the inner diameter and cross-sectional area of the tube, respectively, and f_D shows the Darcy friction factor which was estimated using the model proposed by Churchill [15]:

$$f_D = 8 \times \left[\left(\frac{8}{Re} \right)^{12} + (A+B)^{-1.5} \right]^{\frac{1}{12}}$$
 (A.2)

$$A = \left\{ -2.457 \ln \left[\left(\frac{7}{Re} \right)^{0.9} + 0.27 \left(\frac{e}{2r_{t,in}} \right) \right] \right\}^{16}, B = \left(\frac{37530}{Re} \right)^{16}$$
(A.3)

where Re and e are respectively Reynolds number and surface roughness. In the energy equation (Eq. (A.1)), q'_{wall} is the radial heat transfer from the surroundings to the pipe which was calculated by:

$$q'_{wall} = 2\pi \left[\frac{d_h}{r_{t,in} N u k_t} + \frac{\ln \left(\frac{r_{t,out}}{r_{t,in}} \right)}{k_t} \right]^{-1} \times \left(T_{ext} - T_{cf} \right)$$
(A.4)

where k_t and $r_{t,out}$ are respectively the thermal conductivity and outer radius of tube; d_h is the hydraulic diameter of the tube, T_{ext} is the external temperature, and Nu is the Nusselt number which is given by:

$$Nu = max \left\{ 3.66, \frac{\left(\frac{f_D}{8}\right)(Re - 1000)Pr}{1 + 12.7\left(\frac{f_D}{8}\right)^{0.5}\left(Pr^{\frac{2}{3}} - 1\right)} \right\}$$
(A.5)

where *Pr* is the Prandtl number. It needs to be mentioned that a value of 3.66 for Nu corresponds to the laminar flow regime for a circular section, while the second term corresponds to the turbulent flow.

References

- S.L. Abdelaziz, C.G. Olgun, J.R. Martin, Design and operational considerations of geothermal energy piles, Geo-Front. 2011 (2011) 450–459.
- [2] J. Acuńa, P. Mogensen, B. Palm, Distributed thermal response test on a u-pipe borehole heat exchanger, Appl. Energy 109 (2009).
- [3] M.P. Anderson, Heat as a ground water tracer, Groundwater 43 (2005) 951-968.
- [4] A. Angelotti, L. Alberti, I. La Licata, M. Antelmi, Energy performance and thermal impact of a borehole heat exchanger in a sandy aquifer: influence of the groundwater velocity, Energ. Conver. Manage. 77 (2014) 700–708.
- [5] D. Bauer, W. Heidemann, H. Müller-Steinhagen, H.-J.-G. Diersch, Thermal resistance and capacity models for borehole heat exchangers, Int. J. Energy Res. 35 (2011) 312–320.
- [6] F. Behbehani, J.S. McCartney, Energy pile groups for thermal energy storage in unsaturated soils, Appl. Therm. Eng. 215 (2022), 119028.
- [7] R.A. Beier, Transient heat transfer in a U-tube borehole heat exchanger, Appl Therm. Eng. 62 (2014) 256–266.
- [8] R.A. Beier, S. Morchio, M. Fossa, Thermal response tests on deep boreholes through multiple ground layers, Geothermics 101 (2022), 102371.
- [9] A. Bidarmaghz, G.A. Narsilio, Is natural convection within an aquifer a critical phenomenon in deep borehole heat exchangers' efficiency? Appl. Therm. Eng. 212 (2022), 118450.
- [10] S. Cai, X. Li, M. Zhang, J. Fallon, K. Li, T. Cui, An analytical full-scale model to predict thermal response in boreholes with groundwater advection, Appl. Therm. Eng. 168 (2020), 114828.

- [11] W. Cai, F. Wang, J. Liu, Z. Wang, Z. Ma, Experimental and numerical investigation of heat transfer performance and sustainability of deep borehole heat exchangers coupled with ground source heat pump systems, Appl. Therm. Eng. 149 (2019) 975–986.
- [12] D.Y. Cherati, O. Ghasemi-Fare, Practical approaches for implementation of energy piles in Iran based on the lessons learned from the developed countries experiences. Renew. Sustain. Energy Rev. 140 (2021), 110748.
- [13] A.D. Chiasson, S.J. Rees, J.D. Spitler, A preliminary assessment of the effects of groundwater flow on closed-loop ground source heat pump systems, Oklahoma State Univ, Stillwater, OK (US), 2000.
- [14] J.C. Choi, J. Park, S.R. Lee, Numerical evaluation of the effects of groundwater flow on borehole heat exchanger arrays, Renew. Energy 52 (2013) 230–240.
- [15] Churchill, S.W., 1977. Friction-factor equation spans all fluid-flow regimes.
- [16] N. Diao, Q. Li, Z. Fang, Heat transfer in ground heat exchangers with groundwater advection, Int. J. Therm. Sci. 43 (2004) 1203–1211.
- [17] B.H. Dinh, G.-H. Go, Y.-S. Kim, Performance of a horizontal heat exchanger for ground heat pump system: effects of groundwater level drop with soil–water thermal characteristics, Appl. Therm. Eng. 195 (2021), 117203.
- [18] R. Fan, Y. Jiang, Y. Yao, D. Shiming, Z. Ma, A study on the performance of a geothermal heat exchanger under coupled heat conduction and groundwater advection, Energy 32 (2007) 2199–2209.
- [19] J. Gao, X. Zhang, J. Liu, K. Li, J. Yang, Numerical and experimental assessment of thermal performance of vertical energy piles: an application, Appl. Energy 85 (2008) 901–910.

- [20] O. Ghasemi-Fare, P. Basu, A practical heat transfer model for geothermal piles, Energ. Buildings 66 (2013) 470–479.
- [21] O. Ghasemi-Fare, P. Basu, Predictive assessment of heat exchange performance of geothermal piles, Renew. Energy 86 (2016) 1178–1196.
- [22] O. Ghasemi-Fare, P. Basu, Influences of ground saturation and thermal boundary condition on energy harvesting using geothermal piles, Energ. Build 165 (2018) 340–351.
- [23] O. Ghasemi-Fare, P. Basu, Coupling heat and buoyant fluid flow for thermal performance assessment of geothermal piles, Comput. Geotech. 116 (2019), 103211.
- [24] A.F. Gheysari, H.M. Holländer, P. Maghoul, A. Shalaby, Sustainability, climate resiliency, and mitigation capacity of geothermal heat pump systems in cold regions, Geothermics 91 (2021), 101979.
- [25] J. Gong, Z. Li, W. Zhang, A. Hu, G. Jin, Analysis of thermal interaction coefficient for multiple borehole heat exchangers in layered soil considering groundwater seepage, Appl. Therm. Eng. 207 (2022), 118166.
- [26] D. Hillel, Introduction to soil physics, Academic press, 2013.
- [27] E. Holzbecher, Free and forced convection in porous media open at the top, Heat Mass Transf. 41 (2005) 606–614.
- [28] E. Holzbecher, Y. Yusa, Numerical experiments on free and forced convection in porous media, Int. J. Heat Mass Transf. 38 (1995) 2109–2115.
- [29] M.M. Krol, R.L. Johnson, B.E. Sleep, An analysis of a mixed convection associated with thermal heating in contaminated porous media, Sci. Total Environ. 499 (2014) 7–17.
- [30] E.R. Lapwood, Convection of a fluid in a porous medium, Math. Proc. Camb. Philos. Soc. 44 (1948) 508–521.
- [31] Y. Lou, P.-F. Fang, X.-Y. Xie, C.S.A. Chong, F.-Y. Li, C.-Y. Liu, Z.-J. Wang, D.-Y. Zhu, Numerical research on thermal response for geothermal energy pile groups under groundwater flow, Geomech. Energy Environ. 28 (2021), 100257.
- [32] J.S. McCartney, M. Sánchez, I. Tomac, Energy geotechnics: Advances in subsurface energy recovery, storage, exchange, and waste management, Comput. Geotech. 75 (2016) 244–256.
- [33] N. Mehraeen, M.M. Ahmadi, O. Ghasemi-Fare, Numerical modeling of mixed convection near a vertical heat source in saturated granular soils, Geothermics 106 (2022), 102566.
- [34] A. Mohammadzadeh, F.N. Jazi, O. Ghasemi-Fare, Z. Sun, Analyzing the feasibility of using shallow geothermal energy to prohibit pavement thermal cracking: field testing, Geo-Congress 2023 (2023) 603–611.
- [35] N. Molina-Giraldo, P. Blum, K. Zhu, P. Bayer, Z. Fang, A moving finite line source model to simulate borehole heat exchangers with groundwater advection, Int. J. Therm. Sci. 50 (2011) 2506–2513.
- [36] S. Morchio, M. Fossa, On the ground thermal conductivity estimation with coaxial borehole heat exchangers according to different undisturbed ground temperature profiles, Appl. Therm. Eng. 173 (2020), 115198.
- [37] S. Morchio, M. Fossa, Modelling and validation of a new hybrid scheme for predicting the performance of U-pipe borehole heat exchangers during distributed thermal response test experiments, Appl. Therm. Eng. 186 (2021), 116514.

- [38] S. Morchio, M. Fossa, A. Priarone, A. Boccalatte, Reduced scale experimental modelling of distributed thermal response tests for the estimation of the ground thermal conductivity, Energies 14 (2021) 6955.
- [39] S. Morchio, P. Pasquier, M. Fossa, R.A. Beier, A spectral method aimed at explaining the role of the heat transfer rate when the Infinite Line Source model is applied to Thermal Response Test analyses, Geothermics 111 (2023), 102722.
- [40] T.Y. Ozudogru, O. Ghasemi-Fare, C.G. Olgun, P. Basu, Numerical modeling of vertical geothermal heat exchangers using finite difference and finite element techniques, Geotech. Geol. Eng. 33 (2015) 291–306.
- [41] E.R.d. Schio, S. Lazzari, A. Abbati, Natural convection effects in the heat transfer from a buried pipeline, Appl. Therm. Eng. 102 (2016) 227-233.
- [42] G.R. Shanker, K. Homan, Convective transport from geothermal borehole heat exchangers embedded in a fluid-saturated porous medium, Renew. Energy 196 (2022) 328–342.
- [43] M.H. Sharqawy, H.M. Badr, E.M. Mokheimer, Investigation of buoyancy effects on heat transfer between a vertical borehole heat exchanger and the ground, Geothermics 48 (2013) 52–59.
- [44] H. Sun, X. Qin, X. Yang, Y. Zhao, Study on the heat transfer in different aquifer media with different groundwater velocities during thermal conductive heating, Environ. Sci. Pollut. Res. 27 (2020) 36316–36329.
- [45] M.M. Tamizdoust, O. Ghasemi-Fare, Numerical analysis on feasibility of thermally induced pore fluid flow in saturated soils. Eighth International Conference on Case Histories in Geotechnical Engineering, 2019.
- [46] M.M. Tamizdoust, O. Ghasemi-Fare, A fully coupled thermo-poro-mechanical finite element analysis to predict the thermal pressurization and thermally induced pore fluid flow in soil media, Comput. Geotech. 117 (2020), 103250.
- [47] A.K. Tiwari, P. Basu, Interpretation of TRT data in the presence of natural convection and groundwater flow in saturated ground, Comput. Geotech. 140 (2021), 104426.
- [48] V. Wagner, P. Blum, M. Kübert, P. Bayer, Analytical approach to groundwaterinfluenced thermal response tests of grouted borehole heat exchangers, Geothermics 46 (2013) 22–31.
- [49] H. Wang, C. Qi, H. Du, J. Gu, Thermal performance of borehole heat exchanger under groundwater flow: a case study from Baoding, Energ. Build. 41 (2009) 1368–1373.
- [50] X. Zhai, K. Atefi-Monfared, Local thermal non-equilibrium effects on thermal pressurization in saturated porous media considering thermo-osmosis and thermalfiltration, Comput. Geotech. 126 (2020), 103729.
- [51] J. Zhao, H. Wang, X. Li, C. Dai, Experimental investigation and theoretical model of heat transfer of saturated soil around coaxial ground coupled heat exchanger, Appl. Therm. Eng. 28 (2008) 116–125.
- [52] Z. Zhao, Y.-F. Lin, A. Stumpf, X. Wang, Assessing impacts of groundwater on geothermal heat exchangers: a review of methodology and modeling, Renew. Energy (2022).